Lean female mice producing *trans* 10, *cis* 12-conjugated linoleic acid present excessive fibroblast growth factor 21, adrenaline, and prostaglandin E2

Yu Rao[1,2,#], Lu-Wen Liang[1,#], Mei-Juan Li[3,#], Yang-Yang Wang[1], Bao-Zhu Wang[1], Ke-Mian Gou[1,2,*]

[1]*Institute of Comparative Medicine,* [2]*Jiangsu Co-innovation Center for Prevention and Control of Important Animal Infectious Diseases and Zoonoses, Department of Experimental Zoology, College of Veterinary Medicine, Yangzhou University, Yangzhou 225009, China*;

[3]*Institute of Animal Husbandry and Veterinary Science, Guizhou Academy of Agricultural Sciences, Guiyang 550005, China.*

# These authors contributed equally to this work.

*Corresponding author: Kemian Gou, College of Veterinary Medicine, Yangzhou University, Wenhui South Road, Yangzhou 225009, China.

Email: gou@yzu.edu.cn

ABSTRACT

Dietary *trans* 10, *cis* 12-conjugated linoleic acid (t10c12-CLA) has been shown to induce white fat reduction. In this study, the transgenic mice that produce endogenous t10c12-CLA were used to determine the long-term impact of this substance on lipid metabolism in lean female mammals. Phenotype profiling showed that the t10c12-CLA did not induce fat loss but resulted in less heat release and oxygen consumption, as well as excessive adrenaline, tumour necrosis factor-alpha, and interleukin-6 in either biallelic Pai/Pai or monoallelic Pai/wt mice compared to their wild-type littermates. Furthermore, the following effects of t10c12-CLA were genotype-specific. Pai/wt mice specifically exhibited increased chronic fibroblast growth factor 21 (FGF21) and reduced physical activities. Contrarily, Pai/Pai mice showed the overproduction of prostaglandin E2 (PGE2), corticosterone, and glucagon, accompanied by hypertriglyceridemia and fatty liver. Further analysis of Pai/Pai livers revealed that the steatosis resulted from attenuated lipid metabolism via down-regulating phosphorylated AMP-activated protein kinase (AMPK) and fatty acid synthase. Analysis of Pai/Pai brown adipose tissue indicated stimulated thermogenesis and lipolysis by up-regulating uncoupling proteins 1 and 2, phosphorylated hormone-sensitive lipase, carnitine palmitoyltransferase 1B, and AMPK, as well as down-regulating phosphorylated AMPK. These results suggest that chronic t10c12-CLA may affect lipid metabolism by stimulating the overproduction of multiple hormones (FGF21, PEG2, adrenaline, etc.) in a dose-dependent manner in lean female mammals.

Keywords: conjugated linoleic acid; prostaglandin E2; steatosis; adrenaline; inflammation; brown adipose tissue

41 **1. INTRODUCTION**

42

43 *Trans* 10, *cis* 12-conjugated linoleic acid (t10c12-CLA) occurs naturally in small
44 amounts in foods such as beef and dairy products. Its popular health benefit is reducing body
45 fat by increasing energy expenditure via browning of white adipose tissue (WAT) [1, 2] or
46 uncoupling protein (UCP) 1 & 2-mediated thermogenesis in brown adipose tissue (BAT) [3],
47 promoting biosynthesis of N-lactoyl-phenylalanine via the up-regulation of cytosolic
48 nonspecific dipeptidase 2 in WAT [4], or increasing intramuscular fat [5]. In addition, it has
49 other potential health influences, including protecting against atherosclerosis by modulating
50 the macrophage phenotype [6], promoting beneficial effects on cholesterol efflux [7],
51 reducing oxidative stress [8], changing intestinal microbiota [9] and metabolite profiles [5],
52 even down-regulating Alzheimer's hallmarks in an aluminium mouse through an Nrf2-
53 mediated adaptive response and increasing brain glucose transporter levels [10].

54 Although the potential health benefits, especially the fat loss properties of dietary
55 t10c12-CLA, have been extensively studied in obese animals, the potential health benefits in
56 lean animals have not been clarified fully. A study in lean male mice treated with dietary
57 t10c12-CLA observed a dramatic reduction in fat mass in the first two weeks which
58 interestingly rebounded during the following 3-5 weeks due to a massive accumulation of
59 lipids in the liver [11]. At the same time, other studies have confirmed its fat loss properties
60 but indicated its side effects result in fatty liver in male [9, 11] or female lean mice [12-16].

61 In our previous study, we produced a transgenic mouse that can produce t10c12-
62 CLA after inserting the foreign gene encoding the *Propionibacterium acnes* isomerase (PAI)
63 into the Rosa26 locus [3]. This Rosa26-Pai knock-in mouse exhibited continuous production
64 of t10c12-CLA and can be used to elucidate its enduring influence on overall health. In its
65 lean male offspring, fat reduction in biallelic Pai/Pai, not in monoallelic Pai/wt genotypes
66 suggests t10c12-CLA's impact is dose-dependent. Additionally, low doses of t10c12-CLA
67 possibly play an active role in lipid metabolism by stimulating the fibroblast growth factor
68 21 (FGF21) secretion. Whereas the high doses of t10c12-CLA possibly induce fat reduction
69 by promoting energy expenditure via UCP1/2-mediated BAT thermogenesis [3].

70 The current study continued to investigate the adiposity characteristics and
71 metabolic profiles of these lean female mice. In contrast to their male counterparts, the
72 findings of this study demonstrate that Pai female mice did not experience changes in body
73 fat but did experience a decrease in heat release. Moreover, specific metabolic features in

74 Pai/wt female mice have confirmed that the low doses of t10c12-CLA can induce the
75 overproduction of FGF21, while the high doses of t10c12-CLA stimulate excessive
76 prostaglandin E2 (PGE2), corticosterone, and glucagon which probably affect the lipid
77 metabolism via varies of pathways. The results suggest that Pai mice may be a useful model
78 to investigate the chronic t10c12-CLA's effects and its mechanisms of action in the body.

2. MATERIALS AND METHODS

2. 1. Mice and diet

The transgenic founder from a hybrid embryo of DBA/2 and C57BL/6J was backcrossed to C57BL/6J mice for more than eight generations, and then the monoallelic Pai/wt matings were used to produce the Pai/Pai, Pai/wt, and wild-type (wt) offspring for this study. Genotyping was performed using genomic DNA from tail tissues, with the presence of the Pai gene being assayed by amplifying the 514-bp Pai fragments (forward: 5-taaccatgttcatgccttcttc-3; reverse: 5-caccttgttgtagtgtccgttt-3) and the wt Rosa26 sequence being assayed by amplifying the 605-bp fragments that spanned the insertional site of the Rosa26 locus (forward: 5-ccaaagtcgctctgagttgttatcagt-3; reverse: 5-ggagcgggagaaatggatatgaag-3). PCR amplification was performed for 30 cycles at 94°C for 30 sec, 57°C for 30 sec, and 72°C for 40 sec.

Table 1. Sources of dietary ingredients

Ingredients	Grams	Sources
Lactic casein	200.0	Gansu Hualing Dairy Co. Ltd, Hezuo city, China
L-cystine	3.0	Zhongtuan shihua Food Reagents Co. Ltd, Hangzhou, China
Sucrose	176.8	Jinhuitaiya, Chemcal Reagents Co. Ltd, Tianjin, China
Corn Starch	452.2	Zhucheng Xingmao Corn Co. Ltd, Weifang city, China
Maltodextrin 10	75.0	Dongzhu Food Co. Ltd, Guilin city, China
Cellulose	50.0	Yisheng Kangyuan Biotech Co. Ltd, Zibo city, China
Soybean oil	25.0	Shandong Luhua Co. Ltd, Leiyang, China
Lard	20.0	Yaodong Baofengyuan Co. Ltd, Qingdao, China
Mineral Mix (20x)	50.0	Mingxin Chemical Reagents Co. Ltd, Zhenzhou, China
Choline bitartrate	2.0	Zhejiang Linuo Biotech Co. Ltd, Yiwu, China
Vitamin Mix (1000x)	1.0	Mingxin Chemical Reagents Co. Ltd, Zhenzhou, China
Total Gram	1055	

Mice of the above three genotypes aged 11-15 weeks were used for analysis in this study unless otherwise specified. All animal experiments were conducted in accordance with the guidance provided by the Committee for Experimental Animals of Yangzhou University. The animal study protocol was approved by the Ethics Committee of Yangzhou University (protocol code NSFC2020-SYXY-20 and dated 25 March 2020). The mice were housed in a

light-controlled room (12L:12D, lights on at 0700 h) at a temperature of 22-23°C and fed ad libitum with a standard diet containing 10% kcal% fat. Fresh diets were prepared every month in accordance with formula No. D12450H of OpenSource DIETS™ (Research Diets Inc., NJ, USA) under sterile conditions. The composition of the D12450H and the sources of the food-grade ingredients used in the diets are provided in Table 1.

2. 2. Major methods

The procedures utilised in this study, including gas chromatography, real-time RNA and proteins analyses, histological analysis, intraperitoneal glucose (2g/kg body weight) and insulin (0.5 IU/kg body weight) tolerance tests, hepatic and blood parameter measurements, and experiments conducted in metabolic cages, were performed following the standard methods as described in our previous study of transgenic male mice [3].

2.3. Measurement of serum estradiol

Three-week-old mice were injected intraperitoneally with 5 IU pregnant mare serum gonadotrophin (Jinmu Biotech Co. Ltd., Wuxi, China), and 48 h later, blood was collected from the orbital vein of anaesthetised mice and used to measure the serum estradiol levels using the E2 ELISA kit (Meimian Industrial Co. Ltd., Jiangsu, China).

2. 4. Statistical analysis.

Analysis was conducted using GraphPad Prism 8.0 (GraphPad Software Inc.; La Jolla, CA, USA). Comparisons between wt and Pai/Pai samples were performed using an unpaired two-tailed t-test with Welch's correction where appropriate. Multiple comparisons among wt, Pai/wt, and Pai/Pai groups were performed using one-way ANOVA and Brown-Forsythe and Welch tests. Data are presented as mean ± standard deviation (SD), and $p < 0.05$ was considered statistically significant.

3. RESULTS

3. 1. Fatty acids analysis

Gas chromatography was used to analyse the compositions of fatty acids (FAs) in the livers, kidneys, hearts, tibialis anterior muscle, and interscapular BAT. The content of t10c12-CLA had increased by 69% in the Pai/wt kidneys compared to wt littermates ($p < 0.05$; Table 2). However, the quantities of substrate linoleic acid had decreased in the Pai/Pai livers by 23% and skeletal muscle by 34% and had increased by 36% in the Pai/wt kidneys ($p < 0.05$; Supplementary Table 1).

The contents of other FAs such as myristic (14:0), palmitic (16:0), stearic (18:0), palmitoleic (16:1n-7), cis-vaccenic (18:1n-7), oleic (18:1n-9), arachidonic (20:4n-6), and docosahexaenoic (22:6n-3) acids were changed to varying degrees in one or more tissues (Supplementary Table 1), This suggests that the changes in the content of each FA were genotype- or tissue-specific. Additionally, the amounts of total FAs (mg/g) increased in the Pai/wt kidneys (10.2 ± 1.39 versus 13.3 ± 1.69; $p < 0.05$), similar to our previous study in Pai/wt male mice [3]. These results suggest lipopathy in the Pai/wt kidney.

Table 2. Content comparison of t10c12-CLA (μg/g) in wild-type and Pai mice

	wild-type (n)	Pai/wt (n)	Pai/Pai (n)
Liver	2.56 ± 3.24 (7)	4.30 ± 4.10 (5)	ND (5)
Kidney	6.50 ± 1.25[a] (5)	11.0 ± 3.65[b] (6)	6.09 ± 0.42[a] (4)
Heart	ND (5)	ND (4)	ND (4)
Muscle	ND (4)	ND (4)	ND (4)
Brown adipose tissue	22.4 ± 15.9 (4)	29.5 ± 7.5 (4)	29.8 ± 0.5 (4)

Note: Tissues from 11-week-old mice was analysed by gas chromatography and 19:0 is an internal standard. ND, not detected. Each value represents the mean ± SD and the numbers in brackets indicate the size of the tested samples. Different letters in superscript indicate a level of statistical significance of $p < 0.05$.

3. 2. Growth analysis

There was a significant difference in weaning weight among the three genotypes (wt > Pai/wt > Pai/Pai, respectively; $p < 0.05$; Fig. 1), similar to our previous study in male mice [3]. However, this bodyweight difference disappeared from five weeks of age onwards.

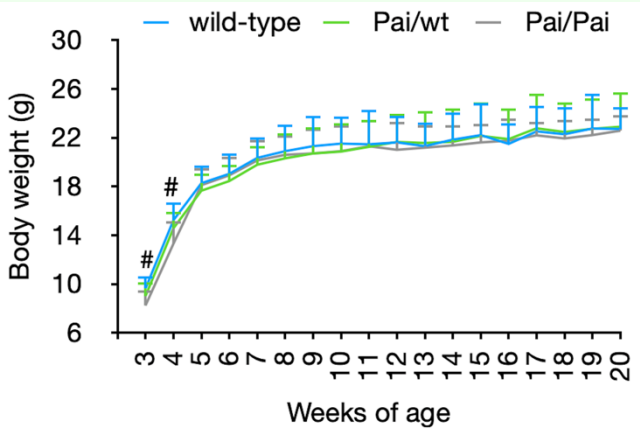

Figure 1. Comparison of growth of wild-type and Pai mice. Each group contained 11-29 mice. Bars represent the mean ± SD. # indicates $p < 0.05$ among three genotypes.

3. 3. Energy metabolism and activity studies

Energy metabolism and activity parameters were assessed in consideration of body weight. Compared to their wt littermates, both Pai/wt and Pai/Pai mice exhibited no significant differences in body weight gain, food and water intake (Fig. 2 A-C), total distance travelled during the whole 72-h observation (Fig. 2 D), and respiratory exchange ratio (Fig. 2 E-F). However, the other parameters showed varying differences.

The Pai/Pai mice covered a longer distance per sampling duration (~50% longer) and exhibited 52.5% higher speed during the light phase ($p < 0.05$; Fig. 2 G-H) but did not decrease their total locomotor activities in either the centre (Fig. 2 I-L) or margin/corners (Fig. 2 M-P). Nevertheless, during both the light ($p < 0.05$) and dark ($p > 0.05$) periods, they consumed 8.9% and 9.2% less O_2 (Fig. 2 Q) and produced 10.8% and 10.1% less CO_2 (Fig. 2 R) as well as 9.3% and 9.4% less heat (Fig. 2 S-T), respectively. The results suggest that Pai/Pai mice simultaneously reduce oxygen consumption and heat release while maintaining normal locomotor activities.

On the other hand, Pai/wt females did not reduce their central activities ($p > 0.05$; Fig. 2 I-L) but displayed 30.1% fewer marginal activities, such as marginal ambulating and stereotypic activities during the dark period ($p < 0.05$; Fig. 2 M-P). Moreover, during both the light and dark periods, they consumed 10.7% and 14.6% less O_2, produced 9.7% and 15.2% less CO_2, as well as 10.5% and 14.7% less heat, respectively ($p < 0.05$, Fig. 2 Q-T), suggesting that Pai/wt mice simultaneously reduce oxygen consumption and heat release while exhibiting fewer marginal activities.

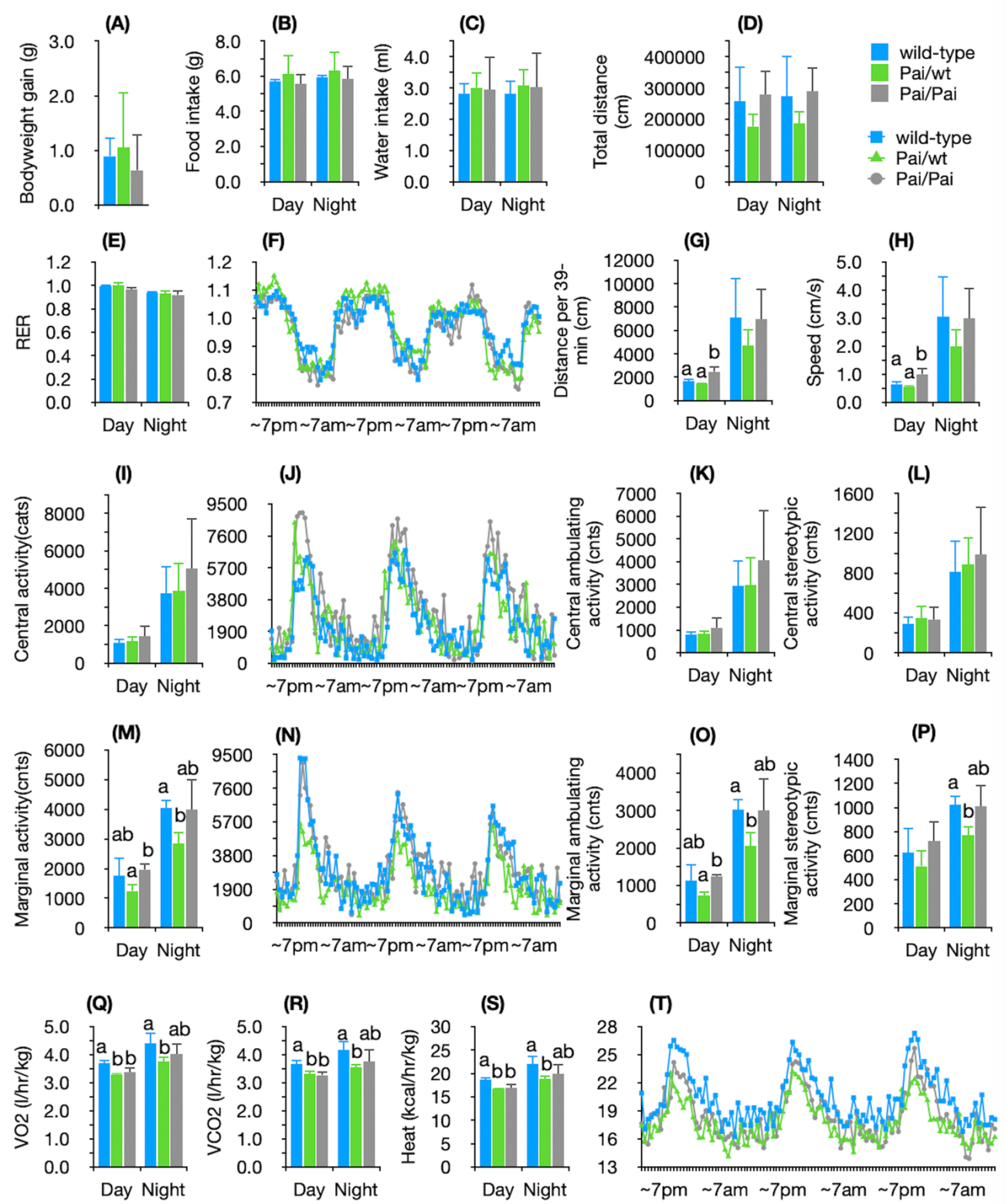

Figure 2. Abnormal energy metabolism and activities in Pai mice. Comparison of body weight gain during a 72-h period (A), food intake (B), water intake (C), total distance travelled during a 72-h period (D), respiratory exchange ratio (RER) and RER time course (E-F), distance travelled during a 39-min sampling duration (G), speed (H), locomotor activities in the centre of the cage and its time course (I-J), central ambulating and stereotypic activities

173 (K-L), locomotor activities in the margin or corners of the cage and its time course (M-N),
174 marginal ambulating and stereotypic activities (O-P), O_2 consumption (Q), CO_2 production
175 (R), heat release and its time course (S-T) among wild-type (n = 4), Pai/wt (n = 4) and Pai/Pai
176 (n = 4) mice at 11 weeks. The lights turned on and off at 7:00 am and 7:00 pm, respectively.
177 The data are normalised to lean body weight. The bars represent the mean ± SD. Different
178 letters indicate $p < 0.05$ within the same phase.

179

180 ***3. 4. Metabolic complications***

181 Concentrations of circulating glucose, insulin, leptin, and ghrelin (Table 3), as well as
182 small intestine length (Supplementary Table 2), showed no significant differences ($p > 0.05$)
183 between Pai mice and their wt littermates. This suggests that t10c12-CLA did not have any
184 significant impact on energy intake, which is consistent with the observation in the metabolic
185 cage.

Table 3. Circulating factors in wild-type and Pai mice

	wild-type (n)	Pai/wt (n)	Pai/Pai (n)
Blood glucose (mM)	7.35 ± 0.70 (12)	7.37 ± 1.18 (15)	7.55 ± 1.35 (13)
Serum insulin (μg/L)	0.21 ± 0.08 (9)	0.27 ± 0.11 (17)	0.32 ± 0.18 (8)
Serum leptin (μg/L)	1.04 ± 0.41 (8)	0.92 ± 0.21 (14)	0.91 ± 0.31 (7)
Serum ghrelin (ng/L)	181 ± 44 (7)	225 ± 108 (20)	210 ± 152 (6)
Serum fibroblast growth factor 21 (ng/L)	403 ± 29^{a} (16)	441 ± 49^{b} (10)	421 ± 34^{ab} (18)
Serum total cholesterol (μM)	311 ± 40 (17)	324 ± 40 (8)	321 ± 30 (16)
Plasma triglycerides (mg/dL)	107 ± 35^{a} (34)	105 ± 27^{a} (29)	129 ± 42^{b} (29)
Plasma high-density lipoprotein (mg/dL)	48.6 ± 13.9 (34)	47.7 ± 16.2 (29)	52.5 ± 19.6 (29)
Serum free fatty acids (μM)	471 ± 95 (8)	527 ± 79 (16)	517 ± 136 (8)
Serum Estradiol (pM)	71.0 ± 8.8 (15)	64.9 ± 6.8 (7)	68.4 ± 8.1 (15)
Serum prostaglandin E2 (ng/L)	349 ± 33^{a} (16)	356 ± 38^{ab} (8)	380 ± 38^{b} (16)
Serum glucagon (mU/L)	54.3 ± 62.3^{a} (20)	55.0 ± 38.4^{a} (17)	104 ± 67^{b} (16)
Serum cortosterone (μg/L)	7.51 ± 1.27^{a} (16)	7.88 ± 1.64^{ab} (8)	8.68 ± 1.61^{b} (16)
Serum adrenaline (μg/L)	3.01 ± 1.64^{a} (7)	10.5 ± 9.4^{b} (14)	13.7 ± 7.5^{b} (7)
Serum interleukin-6 (ng/L)	24.7 ± 17.7^{a} (9)	47.8 ± 27.8^{b} (14)	60.6 ± 32.8^{b} (6)
Serum tumour necrosis factor α (ng/L)	69.1 ± 54.9^{a} (12)	174 ± 161^{b} (16)	205 ± 175^{b} (13)
Serum C reactive protein (μg/L)	34.3 ± 19.2^{a} (16)	49.1 ± 31.4^{a} (17)	107 ± 72^{b} (10)
Serum lactate dehydrogenase (U/L)	2592 ± 646 (7)	2234 ± 627 (7)	2518 ± 454 (6)

Note: Blood samples were collected from non-fasted mice at the ages of 3 (specific for estradiol) or 11~15 weeks. Each value represents the mean ± SD and the numbers in brackets indicate the size of the tested samples. Different letters in superscript indicate a level of statistical significance of $p < 0.05$.

186

187 Although the circulating levels of total cholesterol, free FAs, high-density lipoprotein
188 (HDL), and estradiol showed no significant differences among the three genotypes, the levels
189 of plasma triglycerides (TGs) were significantly elevated in Pai/Pai mice when compared to
190 wt or Pai/wt genotypes ($p < 0.05$, Table 3), indicating hypertriglyceridemia in Pai/Pai mice.

191 In Pai/Pai mice, serum concentrations of prostaglandin E2 (PGE2, 109%), glucagon
192 (2-fold), corticosterone (116%), adrenaline (4.5-fold), tumour necrosis factor-alpha (TNFα, 3-
193 fold), interleukin-6 (IL-6, 2.5-fold), and C-reactive protein (CRP, 3-fold) were significantly
194 increased ($p < 0.05$) when compared to their wt littermates. However, only FGF21 (109%),
195 adrenaline (3.5-fold), TNFα (2.5-fold), and IL-6 (2-fold) were significantly ($p < 0.05$) elevated
196 in Pai/wt mice (Table 3). Additionally, there was no increase in blood levels of lactic acid
197 dehydrogenase in either Pai mice, indicating no cellular injury caused by the PAI protein.
198 These results suggest that the t10c12-CLA can lead to an inflammation reaction and response
199 to illness-related stimuli in female mammals.

200

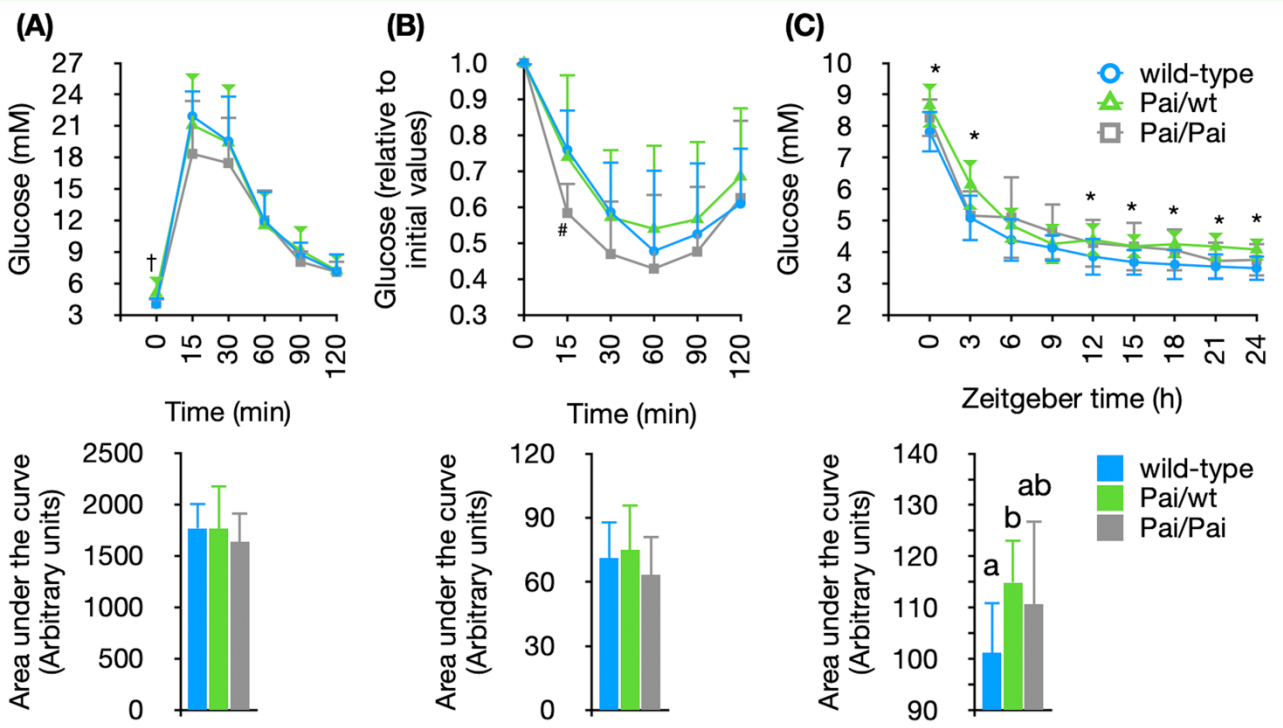

201

202 **Figure 3. Comparisons of glucose (A) and insulin (B) tolerance tests and dynamic glucose**
203 **levels (C) in wild-type (wt) and Pai mice.** (A) Absolute blood glucose levels and the area
204 under the curve are compared among wt (n = 5), Pai/wt (n = 10), and Pai/Pai (n = 5) mice.
205 (B) Blood glucose levels relative to initial values and the area under the curve are compared
206 among wt (n = 10), Pai/wt (n = 12), and Pai/Pai (n = 7) mice. (C) Dynamic blood glucose
207 levels and the area under the curve are measured in wt (n = 12), Pai/wt (n = 13), and
208 Pai/Pai (n = 10) fasting mice starved from Zeitgeber time 0 to 24. Zeitgeber times 0 and 12

are lights-on and -off times, respectively. The bars represent the mean ± SD. † indicates $p < 0.05$ between Pai/wt and wt or Pai/Pai mice; # indicates $p < 0.05$ between wt and Pai/Pai mice; * indicates $p < 0.05$ between wt and Pai/wt mice.

Both glucose and insulin tolerance tests showed no difference in the circulating glucose concentrations or the area under the curve between wt and two Pai genotypes. However, the glucose levels before glucose injection were significantly ($p < 0.05$) higher in Pai/wt mice compared to wt or Pai/Pai littermates (Fig. 3 A-B). To investigate further, we measured blood glucose levels during a 24-h fasting duration and found that Pai/wt mice maintained higher glucose levels continuously compared to their wt littermates ($p < 0.05$; Fig. 3 C). This suggests that t10c12-CLA can ameliorate the circulating glucose level in Pai/wt mice during starvation, which may be associated with the elevated FGF21 exclusively in Pai/wt female mice (Table 3), similar to high FGF21 levels in Pai/wt male mice [3], for its beneficial insulin-sensitising and glucose-lowering effects [17].

3. 5. WAT characteristics

WAT features were determined in the mice at 11 weeks of age. Compared to their wt littermates, Pai/Pai mice showed generalised organomegaly, including significantly enlarged livers, spleens, hearts, and ovaries, when body weight was considered ($p < 0.05$; Supplementary Table 2). However, no fat mass loss was observed (Fig. 4 A-B). The histological analysis did not reveal any changes in the cross-sectional area of white adipocytes (Fig. 4 C-D). Pai/wt mice showed enlarged ovaries only and no fat loss whereas its cross-sectional area per adipocyte was increased ($p < 0.05$), which was also confirmed by the increased mRNA level of leptin (Fig. 4 E).

Total RNA levels of 14 (42%) genes, including seven up-regulated and seven down-regulated, were changed in Pai/Pai white adipocytes among 33 examined genes (Table 4). The seven up-regulated genes were corticosterone receptor Nr3c1, F4/80, Adiponectin, G6p, Fasn, Ppar-γ, and Hsl. The seven down-regulated genes were Lpl, Cpt1a, Plin1, Prdm16, Insr, Glut4, and Chrebp. These aberrant gene expressions in white adipocytes suggest that t10c12-CLA can affect a series of metabolic processes, such as lipid metabolism, lipid and glucose uptake, energy expenditure, stimuli response and glucose homeostasis.

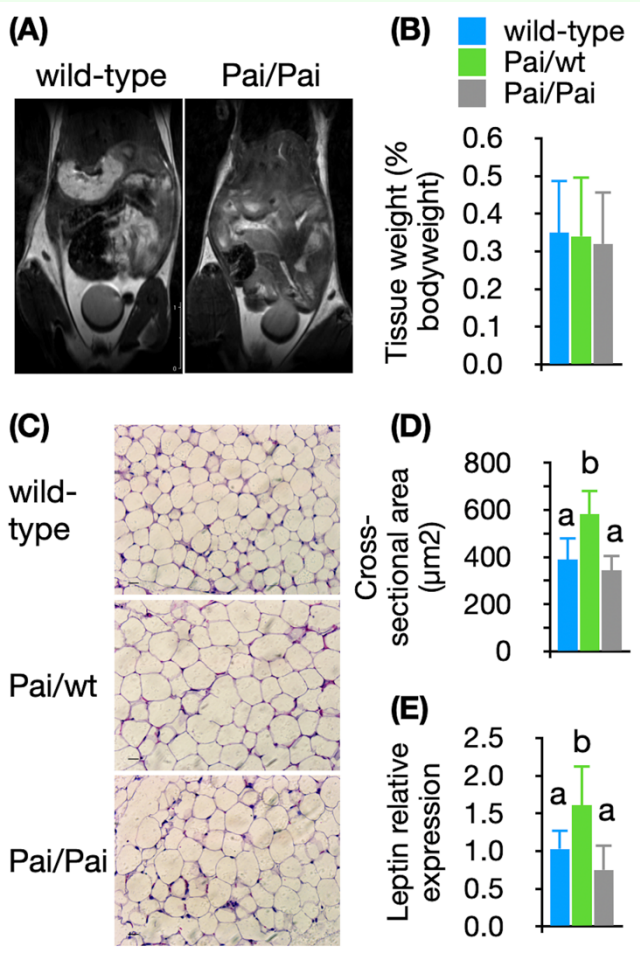

Figure 4. Magnetic resonance imaging and histological analysis of white adipose tissues. (A) Coronal sections were obtained on the whole-body midsection for four wild-type or Pai/Pai mice at 11 weeks in each group during magnetic resonance imaging (bar = 1 cm). The wild-type mice show adipose tissue in the subcutaneous and intra-abdominal regions as areas of increased signal intensity on images. The Pai/Pai mice show normal body fat. (B) There is no difference in WAT mass among wild-type (n = 21), Pai/wt (n = 17), and Pai/Pai (n = 13) mice. (C) Imaging of hematoxylin-eosin staining (bar = 10 μm), (D) analysis of cross-sectional area per cell, and (E) RNA level of leptin gene show that the volume of white adipocytes is specifically increased in Pai/wt mice (n = 5). The bars represent the mean ± SD. Different letters indicate $p < 0.05$.

Similar to Pai/Pai cells, Ppar-γ (1.52 ± 0.34, n = 10), Nr3c1 (1.53 ± 0.21, n = 12), and F4/80 (1.98 ± 0.64, n = 10) were also up-regulated ($p < 0.05$), and Cpt1a (0.58 ± 0.27, n = 5) and Chrebp (0.43 ± 0.45, n = 5) were down-regulated in Pai/wt adipocytes compared to wt samples ($p < 0.05$), respectively. The RNA levels of Fasn and Adiponectin were not different from those of wt samples ($p > 0.05$).

Table 4. Relative Expression of mRNAs in the white adipose tissue

Genes	Wild-type	Pai/Pai
Fatty acid synthase (*Fasn*)	1.04 ± 0.30 (6)	1.80 ± 0.47*** (8)
Peroxisome proliferator-activated receptor-γ (*Ppar-γ*)	1.03 ± 0.24 (12)	1.54 ± 0.61* (10)
Adipose triglyceride lipase (*Atgl*)	1.01 ± 0.16 (7)	1.06 ± 0.19 (7)
Hormone-sensitive lipase (*Hsl*)	1.02 ± 0.23 (9)	1.44 ± 0.29* (8)
Monoacylglycerol lipase (*Mgl*)	0.93 ± 0.25 (9)	0.99 ± 0.32 (8)
Perilipin 1a (*Plin1*)	1.07 ± 0.44 (8)	0.43 ± 0.16** (8)
Comparative gene identification 58 (*Cgi58*)	1.04 ± 0.30 (8)	0.81 ± 0.35 (8)
Lipoprotein lipase (*Lpl*)	1.03 ± 0.27 (14)	0.69 ± 0.24** (15)
Carnitine palmitoyltransferase Ia (*Cpt1a*)	1.06 ± 0.36 (8)	0.56 ± 0.15** (8)
Long-chain acyl-CoA dehydrogenase (*Lcad*)	1.12 ± 0.58 (7)	0.95 ± 0.44 (8)
Medium-chain acyl-CoA dehydrogenase (*Mcad*)	1.01 ± 0.17 (6)	1.07 ± 0.18 (9)
Uncoupling protein 1 (*Ucp1*)	1.09 ± 0.50 (6)	5.39 ± 5.88 (7)
Ppar-gamma coactivator 1 alpha (Pgc1α)	1.05 ± 0.39 (8)	1.18 ± 0.37 (8)
PR domain containing 16 (*Prdm16*)	1.01 ± 0.17 (7)	0.70 ± 0.20** (7)
Insulin receptor (*Insr*)	1.03 ± 0.25 (11)	0.75 ± 0.22** (13)
Insulin receptor substrate-1 (*Irs1*)	0.98 ± 0.32 (15)	1.03 ± 0.34 (20)
Insulin receptor substrate-2 (*Irs2*)	1.17 ± 0.69 (5)	2.28 ± 1.29 (6)
Phosphoinositide 3-kinase (*Pi3k*)	1.05 ± 0.39 (5)	0.78 ± 0.37 (8)
IGF binding protein 1 (*Igfbp1*)	1.80 ± 2.00 (6)	0.55 ± 0.14 (5)
Glucose transporter type 4 (*Glut4*)	1.02 ± 0.24 (6)	0.72 ± 0.17* (6)
Carbohydrate response element binding protein (Chrebp)	1.11 ± 0.51 (8)	0.35 ± 0.17** (8)
Fibroblast growth factor 21 (*Fgf21*)	1.08 ± 0.46 (6)	0.71 ± 0.39 (7)
Glucose-6-phosphatase (*G6p*)	1.24 ± 0.87 (6)	2.68 ± 0.83* (6)
Phosphoenolpyruvate carboxykinase (*Pepck*)	1.07 ± 0.42 (8)	1.11 ± 0.42 (8)
AMP-activated protein kinase (*Ampk*)	1.10 ± 0.49 (5)	1.45 ± 0.58 (8)
Adiponectin	0.99 ± 0.24 (9)	1.42 ± 0.38** (10)
Nuclear receptor subfamily 3 group C member 1 (*Nr3c1*)	1.04 ± 0.29 (22)	1.64 ± 0.81** (22)
F4/80	1.03 ± 0.29 (12)	1.54 ± 0.58* (11)
CD68	1.06 ± 0.38 (14)	1.03 ± 0.61 (13)
CD11c	1.05 ± 0.29 (14)	0.95 ± 0.44 (16)
CCAAT/enhancer-binding-protein beta (*Cebp*)	1.04 ± 0.31 (6)	1.13 ± 0.60 (8)
Forkhead box protein c2 (*Foxc2*)	1.02 ± 0.21 (5)	1.15 ± 0.45 (7)
Pai	1.24 ± 1.23 (23)	393 ± 270*** (25)

Numbers in brackets indicate the size of tested samples. Each value represents the mean ± SD. * indicates $p < 0.05$; ** indicates $p < 0.01$; *** indicates $p < 0.001$, respectively.

257

258 ***3. 6. BAT thermoregulation***

259 To investigate the possible reason for hypothermia in Pai/Pai mice, BAT features
260 were measured. Magnetic resonance imaging and dissection analysis did not reveal any mass
261 changes of BAT in Pai mice (Fig. 5 A-B). HE staining showed Pai/Pai adipocytes with
262 uniform and small-sized lipid drops, while Pai/wt adipocytes had size-irregular lipid drops
263 compared to wt adipocytes containing uniform and large-sized lipid drops (Fig. 5 C). The

264 reduced cross-sectional areas per adipocyte indicated that the volumes of brown adipocytes
265 decreased significantly in both Pai genotypes ($p < 0.05$; Fig. 5 D).

266

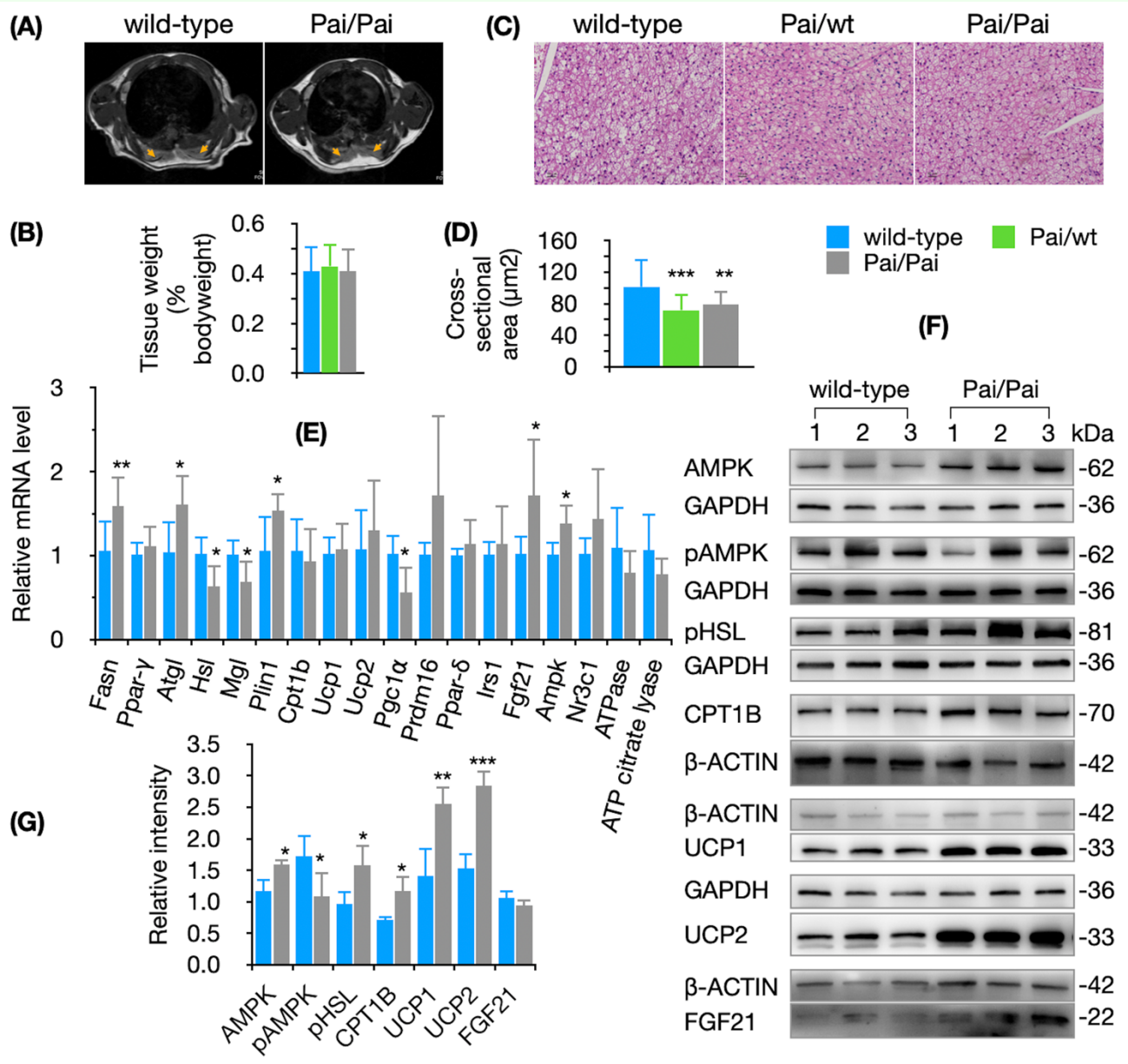

267

268 **Figure 5. Aspects of brown adipose tissues.** (A) Axial sections of the interscapular BAT
269 show similar areas of grey signal intensity on magnetic resonance images (brown arrows)
270 between four Pai/Pai and four wild-type mice at 11 weeks. (B) There is no BAT mass
271 difference among wild-type (n = 21), Pai/wt (n = 17), and Pai/Pai (n = 13) mice. (C-D)
272 Analysis of hematoxylin-eosin staining shows that the sizes of lipid drops become small in
273 the Pai/wt or Pai/Pai adipocytes (bar = 10 μm) and the cross-sectional area per cell is
274 decreased in Pai/wt and Pai/Pai mice (n = 5). (E) Analyses of the relative expression of
275 mRNAs of critical genes in wild-type (n = 5~6) and in Pai/Pai (n = 6~8) mice. (F-G) Western

276 blot analysis of proteins and their relative intensities in wild-type (n = 3) and Pai/Pai mice
277 (n = 3). The full name of the gene/proteins is listed in Table 4. pAMPK, phosphorylated
278 AMPK; pHSL, phosphorylated hormone-sensitive lipase. The bars represent the mean ± SD.
279 * indicates $p < 0.05$; ** indicates $p < 0.01$; and *** indicates $p < 0.001$ vs. wild-type, respectively.

280

281 In Pai/Pai brown adipocytes, among the 18 tested genes, the transcriptional levels
282 were changed in eight genes, which were up-regulated Fasn, Atgl, Plin1, Fgf21, and Ampk;
283 as well as down-regulated Hsl, Mgl, and Pgc1α ($p < 0.05$; Fig. 5 E). In contrast, the other
284 critical genes involved in lipolysis and thermogenesis, such as Ppar-γ, Ucp1, Ucp2, Prdm16,
285 and Ppar-δ, showed no changes in RNA levels. Western blot analysis revealed that UCP1
286 and UCP2, phosphorylated HSL and CPT1B were over-expressed ($p < 0.05$; Fig. 5 F-G).
287 Simultaneously, an increase in total AMPK and a decrease in phosphorylated AMPK were
288 observed in Pai/Pai BAT. These results indicate that the t10c12-CLA effect is associated with
289 BAT's thermogenesis, lipolysis, and beta-oxidation processes. The discrepancy of levels of
290 some mRNA and their encoded proteins also suggests the complex regulation by feedback
291 or adaptive response.

292

293 ***3. 7. Hepatic features***

294 To investigate if t10c12-CLA affects hepatic function, we compared the Pai liver
295 features and the molecular basis of lipid and glucose metabolism with wt samples.

296 In Pai/Pai mice, hepatic hypertrophy was observed (Fig. 6 A). The levels of hepatic
297 TC remained unchanged (Fig. 6 B), but the transcriptional levels of critical genes involved in
298 the sterol pathway were changed, which were down-regulated Srebp1a, Insig2, Hmgcr, and
299 Ldlr; as well as up-regulated Srebp1c and Insig1 ($p < 0.05$; Table 5). On the other hand, the
300 levels of hepatic TGs increased by 15.4%, and histological staining showed profound fat
301 accumulation (~2.3 fold) in swollen hepatocytes ($p < 0.05$; Fig. 6 C-G), indicating hepatic
302 steatosis in Pai/Pai mice. RNA levels of 48% (11/23) genes involved in lipid metabolism were
303 significantly ($p < 0.05$) altered in Pai/Pai livers, including three up-regulated (Fasn, Mgl,
304 Cgi58) and eight down-regulated genes, which were down-regulate Ppar-γ, Dgat1, Dgat2,
305 Atgl, Lpl, Cpt1a, Mcad, and Acox1; as well as up-regulated Mgl and Cgi58 (Table 5). Western
306 blot analysis revealed that the protein levels of pAMPK and FASN were reduced, and CPT1A
307 was increased while the levels of AMPK, ATGL, and CPA1B did not change (Fig. 6 H-I). The
308 result indicates that the chronic effect of t10c12-CLA attenuates the pathway modified by

309 pAMPK. It also suggests that hepatic steatosis causes the down-regulation of fatty acid
310 synthesis and up-regulation of beta-oxidation through negative feedback regulation in the
311 liver.

312

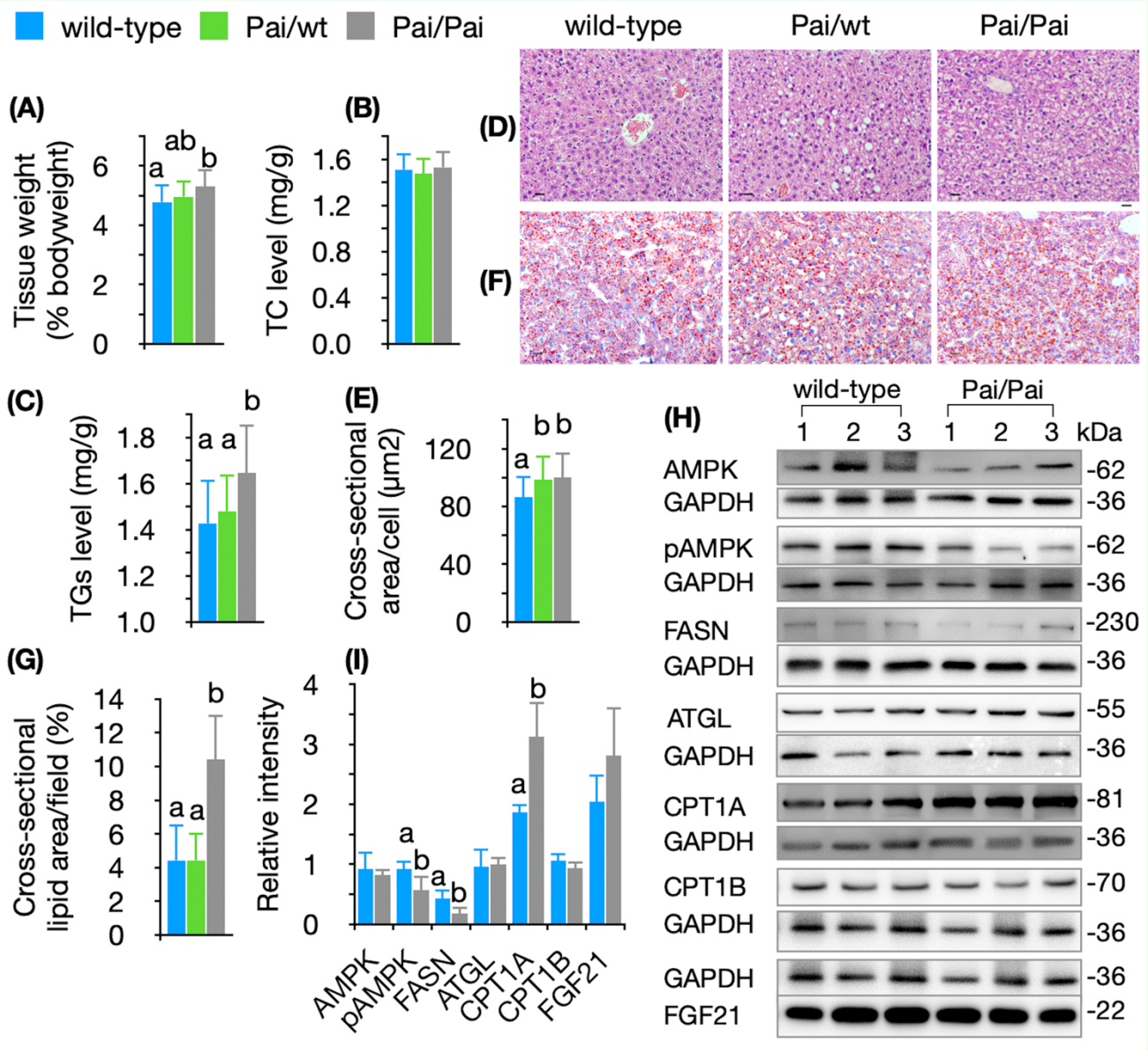

313

314 **Figure 6. Lipid and histological analysis of livers.** (A) Dissection analysis shows an
315 increased liver mass in Pai/Pai (n = 13) but not in Pai/wt (n = 17) mice compared to wild-
316 type mice (n = 21). (B-C) ELISA analyses indicate similar levels of hepatic total cholesterol
317 (TC) and increased levels of triglycerides (TGs) in Pai/Pai livers (n = 12) compared to wild-
318 type (n = 14) and Pai/wt (n = 14). (D-E) Analyses of hematoxylin-eosin staining show the
319 abnormal morphology and hepatocyte oedema in Pai/Pai livers and the enlarged cross-
320 sectional area per cell in Pai/Pai and Pai/wt hepatocytes compared to wild-type samples (n

321 = 5). (F-G) Analyses of Oil red staining show hepatic lipid accumulation in Pai/Pai but not
322 in Pai/wt mice compared to wild-type mice (n = 5), Bar = 10 μm. (H-I) Western blot analysis
323 of proteins and their relative intensities in wild-type (n=3) and Pai/Pai mice (n = 3). The bars
324 represent the mean ± SD, and different letters indicate $p < 0.05$.

325

326 Moreover, this study analysed a range of crucial enzymes related to insulin/IGF
327 signalling and glucose metabolism. The mRNA levels of Igfbp1, Glut4, Fgf21, G6p, and Pepck
328 were decreased, but western blot analysis showed that the FGF21 level did not alter. These
329 findings suggest that t10c12-CLA may have a significant impact on glucose metabolism and
330 insulin sensitivity at least on transcriptional levels in female livers. Additionally, two
331 NADPH-producing enzymes, Malic and Pgd, were significantly up-regulated, and the
332 inflammatory factor CD11c was down-regulated in the Pai/Pai livers ($p < 0.05$; Table 5).

333

Table 5. Relative Expression of mRNAs in the liver

Genes	**wild-type**	**Pai/wt**	**Pai/Pai**
Sterol pathway			
Liver X receptor α (*Lxr*α)	1.00 ± 0.09 (6)	0.91 ± 0.26 (6)	1.08 ± 0.45 (8)
Liver X receptor β (*Lxr*β)	1.04 ± 0.31 (9)	0.91 ± 0.42 (6)	1.11 ± 0.26 (7)
SREBP cleavage-activating protein (*Scap*)	1.01 ± 0.15 (8)	0.92 ± 0.15 (6)	0.90 ± 0.25 (6)
Sterol Regulatory Element Binding Protein-1a (*Srebp1a*)	1.02 ± 0.22^{a} (7)	0.46 ± 0.25^{b} (6)	0.61 ± 0.20^{b} (7)
Srebp1c	0.96 ± 0.33^{a} (6)	1.61 ± 0.55^{b} (7)	1.60 ± 0.42^{b} (5)
Srebp2	1.07 ± 0.39 (8)	1.06 ± 0.22 (7)	1.25 ± 0.52 (8)
Insulin induced gene 1 (*Insig1*)	1.03 ± 0.25^{a} (7)	1.97 ± 0.52^{b} (7)	1.47 ± 0.26^{b} (5)
Insulin induced gene 2a (*Insig2*)	1.07 ± 0.38^{a} (6)	0.20 ± 0.34^{b} (6)	0.59 ± 0.31^{b} (5)
HMG-CoA reductase (*Hmgcr*)	1.01 ± 0.16^{a} (6)	1.23 ± 0.32^{a} (5)	0.62 ± 0.34^{b} (6)
LDL receptor (*Ldlr*)	1.04 ± 0.33^{a} (8)	1.23 ± 0.36^{a} (6)	0.71 ± 0.10^{b} (5)
Fatty acid and TGs synthesis			
Fatty acid synthase (*Fasn*)	1.01 ± 0.18^{a} (6)		2.65 ± 1.32^{b} (6)
Stearoyl-CoA desaturase 1 (*Scd1*)	1.07 ± 0.43 (7)	0.97 ± 0.49 (6)	1.11 ± 0.57 (6)
Peroxisome proliferator-activated receptor-γ (*Ppar-*γ)	1.01 ± 0.46^{a} (14)	1.06 ± 0.27^{a} (7)	0.66 ± 0.44^{b} (12)
Glycerol-3-phosphate acyltransferase 1 (*Gpat1*)	1.04 ± 0.33 (7)	1.44 ± 0.46 (6)	1.22 ± 0.31 (6)
1-acylglycerol-3-phosphate O-acyltransferase 2 (*Agpat2*)	0.97 ± 0.25 (8)	0.80 ± 0.22 (6)	1.11 ± 0.31 (7)
Diacylglycerol acyltransferase-1 (*Dgat1*)	1.00 ± 0.16^{a} (7)	0.81 ± 0.18^{ab} (6)	0.70 ± 0.13^{b} (7)
Diacylglycerol acyltransferase-2 (*Dgat2*)	1.00 ± 0.08^{a} (6)	1.04 ± 0.15^{a} (6)	0.85 ± 0.11^{b} (5)
CD36 (Cd36)	1.06 ± 0.41 (6)		0.83 ± 0.31 (6)

Table 5. Relative Expression of mRNAs in the liver

Genes	wild-type	Pai/wt	Pai/Pai
Lipolysis and fatty acid oxidation			
Hepatic triglyceride lipase (*Htgl*)	0.98 ± 0.27 (7)	0.90 ± 0.28 (6)	1.13 ± 0.34 (7)
Adipose triglyceride lipase (*Atgl*)	1.02 ± 0.21[a] (6)	0.79 ± 0.36[ab] (6)	0.56 ± 0.14[b] (6)
Hormone-sensitive lipase (*Hsl*)	1.05 ± 0.33 (8)	1.29 ± 0.41 (6)	1.16 ± 0.49 (8)
Monoacylglycerol lipase (*Mgl*)	1.02 ± 0.19[a] (8)	1.65 ± 0.55[b] (6)	1.56 ± 0.58[b] (7)
Comparative gene identification 58 (*Cgi58*)	1.05 ± 0.34[a] (7)	1.38 ± 0.66[ab] (6)	1.75 ± 0.59[b] (7)
Adenylate cyclase 3 (*Adcy3*)	1.07 ± 0.42 (8)		1.08 ± 0.23 (8)
Lipoprotein lipase (*Lpl*)	1.02 ± 0.23[a] (7)	0.60 ± 0.17[b] (6)	0.50 ± 0.23[b] (6)
Carnitine palmitoyltransferase Ia (*Cpt1a*)	1.01 ± 0.19[a] (14)	0.83 ± 0.17[b] (7)	0.68 ± 0.18[b] (11)
Long-chain 3-hydroxyacyl-CoA dehydrogenase (*Lchad*)	1.04 ± 0.28 (9)		1.01 ± 0.25 (9)
Acetyl-CoA acyltransferase 2 (*Acaa2*)	1.08 ± 0.44 (7)		1.23 ± 0.23 (6)
Long-chain acyl-CoA dehydrogenase (*Lcad*)	1.00 ± 0.09 (8)	0.93 ± 0.22 (7)	0.78 ± 0.30 (8)
Medium-chain acyl-CoA dehydrogenase (*Mcad*)	1.03 ± 0.27[a] (9)	0.57 ± 0.12[b] (6)	0.65 ± 0.20[b] (6)
Uncoupling protein 1 (*Ucp1*)	1.04 ± 0.32 (7)	1.12 ± 0.40 (7)	0.98 ± 0.34 (7)
Acyl-CoA oxidase-1 (*Acox1*)	1.04 ± 0.32[a] (8)	0.89 ± 0.32[a] (7)	0.69 ± 0.32[b] (8)
Acyl-CoA oxidase-2 (*Acox2*)	1.07 ± 0.42 (9)		1.17 ± 0.43 (9)
Insulin and IGF-1 signaling			
Insulin receptor (*Insr*)	1.05 ± 0.37 (9)	1.35 ± 0.42 (6)	1.36 ± 0.70 (8)
Insulin receptor substrate-1 (*Irs1*)	0.97 ± 0.43 (6)	0.97 ± 0.43 (4)	0.94 ± 0.59 (6)
Insulin receptor substrate-2 (*Irs2*)	1.27 ± 1.01 (9)	1.27 ± 0.87 (7)	1.41 ± 0.99 (8)
Phosphoinositide 3-kinase (*Pi3k*)	1.04 ± 0.28 (7)		1.17 ± 0.24 (7)
Insulin-like growth factor-1 (*Igf1*)	1.04 ± 0.31[a] (8)	1.16 ± 0.29[a] (7)	2.09 ± 0.80[b] (6)
IGF binding protein 1 (*Igfbp1*)	1.04 ± 0.30[a] (6)	0.45 ± 0.33[b] (6)	0.09 ± 0.02[b] (5)
Forkhead box protein a2 (*Foxa2*)	1.06 ± 0.37[a] (9)	1.98 ± 0.86[b] (6)	1.76 ± 0.48[b] (7)
Glucose metabolism and gluconeogenesis			
Glucose transporter type 4 (*Glut4*)	1.06 ± 0.38[a] (6)	0.88 ± 0.28[a] (5)	0.61 ± 0.25[b] (6)
Carbohydrate response element binding protein (*Chrebp*)	1.03 ± 0.26 (5)		1.33 ± 0.43 (6)
Fibroblast growth factor 21 (*Fgf21*)	1.07 ± 0.46[a] (5)		0.19 ± 0.12[b] (7)
Glucose-6-phosphatase (*G6p*)	1.07 ± 0.41[a] (9)	0.47 ± 0.17[b] (7)	0.66 ± 0.19[b] (6)
Phosphoenolpyruvate carboxykinase (*Pepck*)	1.04 ± 0.29[a] (8)	0.53 ± 0.22[b] (6)	0.51 ± 0.19[b] (7)
NADPH-producing			
Malic enzyme (*Malic*)	0.99 ± 0.32[a] (8)	0.98 ± 0.39[a] (7)	1.72 ± 0.70[b] (7)
Glucose-6-phosphate dehydrogenase (*G6pd*)	1.06 ± 0.38 (6)	1.14 ± 0.34 (4)	1.05 ± 0.46 (4)
6-Phosphogluconate dehydrogenase (*Pgd*)	1.05 ± 0.35[a] (7)		1.73 ± 0.56[b] (6)
Others			
AMP-activated protein kinase (*Ampk*)	1.07 ± 0.41 (7)		1.48 ± 0.32 (7)
Liver kinase B1 (*Lkb1*)	1.02 ± 0.23 (5)		1.10 ± 0.12 (5)
Nuclear receptor subfamily 3 group C member 1 (*Nr3c1*)	1.07 ± 0.39 (6)		2.01 ± 1.05 (6)

Table 5. Relative Expression of mRNAs in the liver

Genes	wild-type	Pai/wt	Pai/Pai
CD11c	1.04 ± 0.31^{a} (7)	0.57 ± 0.26^{b} (6)	0.53 ± 0.27^{b} (7)
Cyclophilin	1.01 ± 0.17 (9)	1.04 ± 0.28 (6)	1.01 ± 0.16 (6)
Pai	1.01 ± 0.43^{a} (5)	1674 ± 569^{b} (6)	6059 ± 2317^{c} (6)

Numbers in brackets indicate the size of tested samples. Each value represents the mean ± SD. Different letters in superscript indicate $p < 0.05$.

334

335 Compared to wt samples, Pai/wt livers exhibited normal except for swollen cells
336 (Fig. 6 E). However, among the forty tested genes (Table 5), the mRNA levels of eight genes
337 (Hmgcr, Ldlr, Ppar-γ, Dgat2, Acox1, Igf1, Glut4, and Malic) were significantly ($p < 0.05$)
338 different from those in Pai/Pai livers, but not different from those in wt samples. The
339 remaining 32 genes had similar transcription levels to Pai/Pai samples, and 13 (33%) of them
340 were markedly different from those in wt samples ($p < 0.05$). Specifically, these 13 genes that
341 exhibited different expressions from wt livers included four up-regulated (Mgl, Srebp1c,
342 Insig1, and Foxa2) and nine down-regulated (Lpl, Cpt1a, Mcad, Srebp1a, Insig2, Igfbp1, G6p,
343 Pepck, and Cd11c). These results suggest that gene expression is genotype-specific and that
344 the process of lipolysis and gluconeogenesis is impaired in Pai/wt mice.

345

346 ***3. 8. Hypothalamic analysis***

347 To determine whether t10c12-CLA affected the hypothalamus, critical hypothalamic
348 genes and proteins were also measured. The mRNA levels of the leptin receptor and agouti-
349 related peptide were increased, while the transcription levels of the ghrelin receptor and
350 Orexins decreased in the Pai/wt or Pai/Pai hypothalamus when compared to wt mice (Fig.
351 7 A). Western blot analysis revealed no changes in AMPK, phosphorylated AMPK, and
352 GRP78 proteins in the Pai/Pai hypothalamus; additionally, the ratio of pAMPK/AMPK did
353 not show a significant difference between wt and Pai/Pai samples ($p > 0.05$; Fig. 7 B-C). These
354 findings suggest that the central regulation of energy intake may only be affected at the
355 transcriptional level.

356

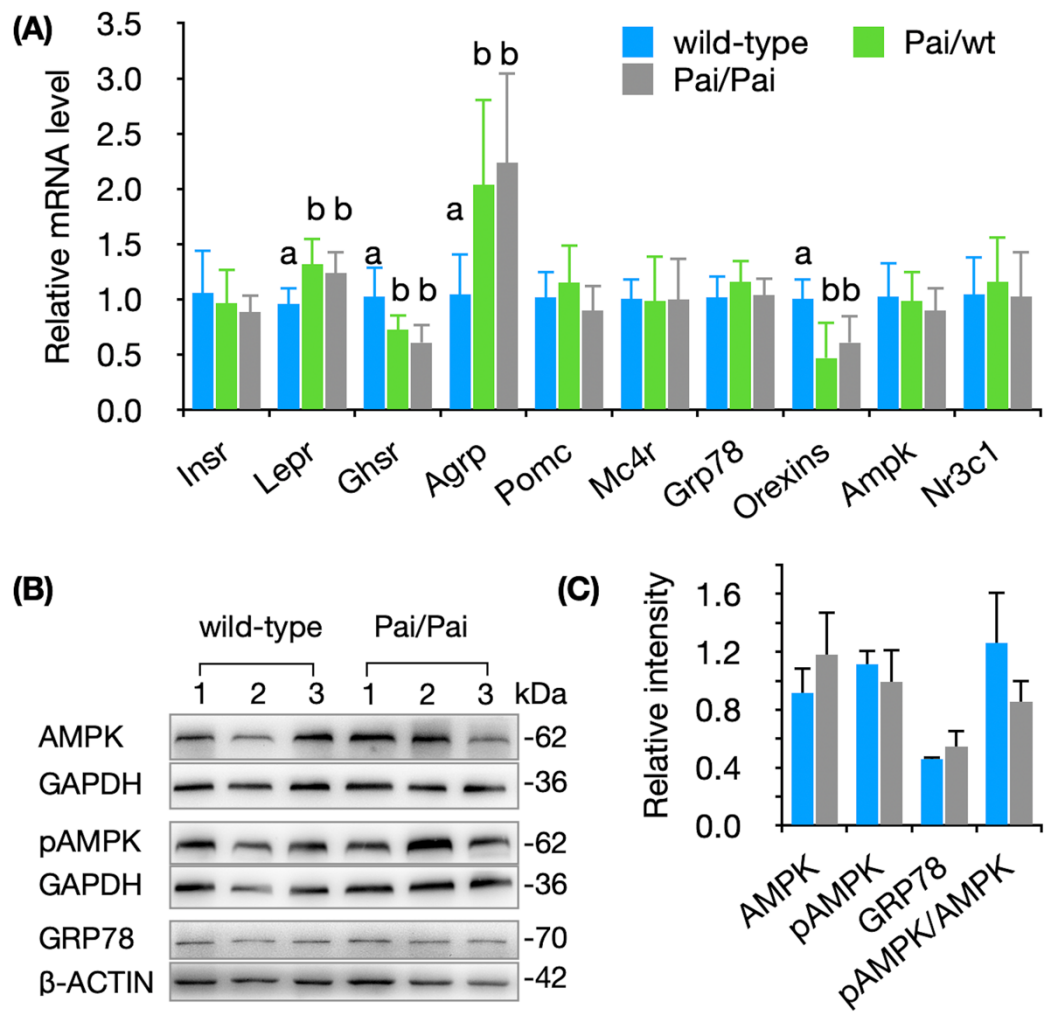

Figure 7. Analyses of the relative mRNAs (A), protein levels and their relative intensities in the hypothalamus (B-C). Agrp, Agouti-related peptide; Ampk, AMP-activated protein kinase; Ghsr, Ghrelin receptor; Grp78, glucose-regulated protein 78; Insr, Insulin receptor; Lepr, Leptin receptor; Mc4r, Melanocortic 4 receptor; Nr3c1, Nuclear receptor subfamily 3 group C member 1; (p)AMPK, (phosphorylated) AMP-activated protein kinase; Pomc, Proopiomelanocortin. The sample sizes for RNA analysis are 6~9 in each group. The bars represent the mean ± SD, and different letters indicate $p < 0.05$.

365 **4. DISCUSSION**

366

367 Our previous observation in Pai/Pai male mice showed that t10c12-CLA reduced
368 body fat by releasing heat via BAT activation with lower blood TGs [3]. Conversely, in the
369 Pai female mice, t10c12-CLA did not cause body fat loss but resulted in complicated
370 symptoms, including hypothermia, fatty liver and hypertriglyceridemia, and was highly
371 responsive to stress and inflammation in a dose-dependent manner. The different
372 physiological and pathological characteristics of both sexes can help us understand the
373 mechanism of action of t10c12-CLA in gender-specific and dose-dependent manners. As for
374 Pai mice, there are two problems we have not fixed until now. Firstly, we have reported as
375 many results as possible for a comprehensive understanding of the Pai mouse, but a few
376 parameters are difficult to explain well and even show contradictions in some respects.
377 Secondly, explaining why there are only minimal differences in t10c12-CLA and linoleic acid
378 is challenging although we once observed drastic changes in an increase of product t10c12-
379 CLA and a decrease of substrate linoleic acid in Pai-transfected 3T3 cells [18].

380 The metabolic pathway of t10c12-CLA, similar to that of linoleic or alpha-linolenic
381 acids [18], suggests it can competitively interrupt the metabolic pathway of n-6 or n-3 FAs
382 and their derived leukotrienes signals/hormonal molecules. It also indicates that t10c12-CLA
383 can be directly converted into the analogues of n-6 FAs and their derivatives. PGE2, an
384 arachidonic acid-derived hormone, will be easily disturbed by t10c12-CLA. PGE2 is involved
385 in stress response and has essential effects on inflammation, fever, and renal filtration [19]. It
386 can induce corticosterone secretion by regulating the hypothalamic-pituitary-adrenal axis
387 activity and enhancing adrenaline synthesis in the Chromaffin cells of the adrenal medulla.
388 Subsequently, the increased circulating corticosterone and adrenaline could stimulate excess
389 glucagon secretion [20]. In Pai/Pai female mice, we have observed the excess PGE2 induced
390 by t10c12-CLA, and then the PGE2 (or analogues) caused the increases in corticosterone,
391 glucagon, adrenaline, and inflammatory factors (IL-6, TNFα, and CRP). Obviously,
392 hypothermia in Pai/Pai female mice may be related to hyperprostaglandinemia,
393 hyperadrenerginemia and inflammatory response; while hyperglyceridemia and fatty liver
394 are associated with hypercorticosteroidemia and glucagon resistance.

395 In the hypothalamic preoptic area, PGE2 receptors EP3, coupled to cAMP decreases,
396 can stimulate a passive defence mechanism such as less O_2 consumption and hypothermia to
397 avoid further energy expenditure; while receptors EP4, connected to cAMP increases, can

398 stimulate an active defence mechanism, including more O_2 consumption and febrile
399 responses by increasing BAT thermogenesis, typically occurs to promote well-being and
400 survival [19, 21]. It suggests that gender-based differences in PGE2 levels might partially
401 result in the opposite heat release in male and female Pai/Pai mice. In female mice, the co-
402 elevation of PGE2 and corticosterone suggests that t10c12-CLA induced a passive defence
403 mechanism including hypothermia which conversely promotes BAT thermogenesis and
404 lipid metabolism by negative feedback to down-regulate pAMPK and up-regulate UCP1,
405 UCP2, CPT1B, and pHSL. In contrast, in male mice, the lack of PGE2 elevation suggests that
406 t10c12-CLA induced an active defence mechanism including hyperthermia to promote
407 survival [3].

408 In addition to PGE2- and adrenaline-induced heating [22], BAT thermogenesis can
409 be mediated through the central GRP78 [23, 24] or AMPK-OREXINS-BMP8B pathway [25].
410 Orexin-null mice exhibited periods of decreased activity during the dark phase and
411 demonstrated hypothermia, reduced oxygen consumption, and blunted thermogenic
412 responses [26]; furthermore, BMP8B's thermogenic effect is sexually dimorphic and observed
413 in females only [25]. The Pai/Pai female mice exhibited similar phenotypes to orexin-null
414 mice and lower transcription levels of Orexins in the Pai hypothalamus. These characteristics
415 suggest that the t10c12-CLA-induced BAT thermogenesis may be regulated through central
416 pathways in female mice. Unfortunately, we did not observe evident changes in GRP78,
417 AMPK, pAMPK, and pAMPK/AMPK ratio in the hypothalamus.

418 Previous studies on mice have yielded conflicting results on whether dietary t10c12-
419 CLA leads to hepatic steatosis [11, 16, 27, 28]. The current observation of fatty liver and
420 hypertriglyceridemia in Pai/Pai mice, which may be associated with t10c12-CLA-induced
421 excess corticosterone for the overproduction of corticosterone can lead to Cushing syndrome,
422 corticosteroid-induced lipodystrophy, hypertriglyceridemia, or hepatic steatosis [29, 30]. On
423 the other hand, the existence of glucagon resistance can increase liver fat [31-33], although
424 chronic increases in plasma glucagon promote lipolysis through INSP3R1/CAMKII/ATGL
425 [34] or PKA/HSL pathways in hepatocytes [35] and stimulate beta-oxidation by activating
426 AMPK/PPAR-α/CPT1A/MCAD pathway [20]. In the current study, the serum glucagon
427 concentration increased nearly twofold in Pai/Pai female mice, which is similar to its
428 physiological levels (2~3 fold) in response to long-term fasting or hypoglycemia [36],
429 whereas the protein levels of unchanged ATGL, decreased pAMPK, and increased CPT1A
430 indicate the chronic glucagon excess did not stimulate the lipolysis and beta-oxidation in the
431 liver. These results suggest that the chronic impact of t10c12-CLA might give rise to glucagon

432 resistance in Pai/Pai female mice. In this case, the down-regulated hepatic enzymes may not
433 fully and immediately catalyse the FAs molecules mobilised from other tissues based on
434 glucagon stimulation. Consequently, it disrupts hepatic and systemic lipid homeostasis and
435 leads to dyslipidemia and fatty liver in female mice. Contrarily, the t10c12-CLA did not cause
436 the overproduction of corticosterone or glucagon in Pai/Pai male mice. Thus, the mice had
437 no fatty liver disease and even exhibited lower TGs levels in the blood.

438 FGF21 is a key regulator of the specific hormonal signalling pathway in increasing
439 energy expenditure, reducing hepatic and plasma TGs levels, accelerating lipoprotein
440 catabolism in WAT and BAT [37], and suppressing physical activity via central action [38].
441 FGF21 signalling enhances insulin sensitivity and lowers serum glucose by acting directly on
442 adipose tissues [17, 39]. The Pai/wt mouse is the first animal in which t10c12-CLA can induce
443 FGF21 secretion. Excess FGF21 is a unique feature in Pai/wt, not in Pai/Pai genotypes,
444 indicating that t10c12-CLA-induced FGF21 secretion is specifically associated with low doses
445 in both genders and it can be suppressed to the normal levels through negative feedback
446 when high doses occur in Pai/Pai mice. This suggests that the health benefits of low-dose
447 t10c12-CLA may be due, in part, to its ability to stimulate FGF21 secretion. Therefore, the
448 different effects of t10c12-CLA on glucose metabolism in diabetic Zucker fatty rats [40] and
449 insulin resistance in mice [12, 41] may be related to the different levels of FGF21 induced by
450 t10c12-CLA. In the current study, excess FGF21 may be associated with specific phenotypes
451 in Pai/wt mice, such as blood glucose homeostasis during starvation, enlarged white
452 adipocytes, no steatosis in hepatocytes and normal circulating TGs. The exact mechanism by
453 which t10c12-CLA activates FGF21 secretion remains unclear and requires further
454 investigation.

455 Based on the excesses of hormones, abnormality of the energy metabolism, and
456 physical activities in Pai/Pai mice in this study, we suggest that high doses of t10c12 result
457 in an increased PEG2 which subsequently induces increases in corticosterone, glucagon, and
458 adrenaline, and inflammatory factors (IL6, TNFα, and C reaction protein). The combination
459 of these factors causes metabolic syndrome, including fatty liver, hyperglyceridemia,
460 hypothermia, and inflammatory changes in lean female mice (Fig. 8). Conversely, low doses
461 of t10c12-CLA may cause increases in circulating adrenaline which can induce WAT lipolysis
462 and BAT heating through a mechanism of negative feedback, and FGF21 which can promote
463 energy expenditure, reduce hepatic and plasma TGs levels, accelerate lipoprotein catabolism
464 in adipocytes, suppress physical activity, and enhance insulin sensitivity and lower serum
465 glucose (Fig. 8).

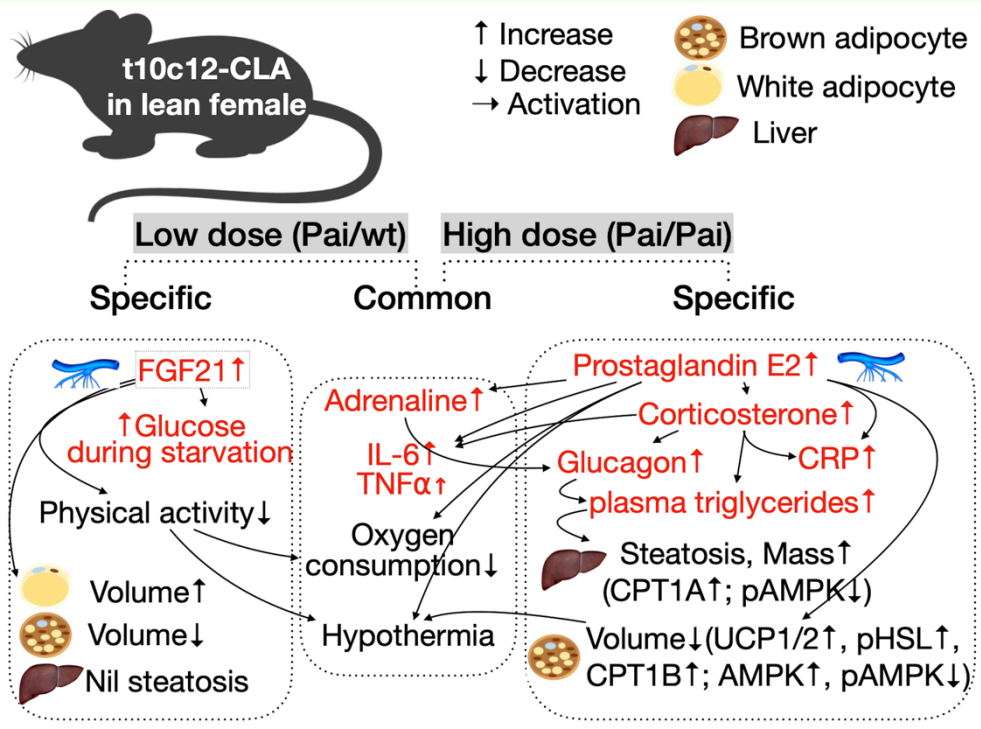

Figure 8. Diagram showing the dose-dependent effect of chronic t10c12-CLA on lean female mice. Besides the common effects, such as increased adrenaline, IL-6, and TNFα, as well as decreased heat release and oxygen consumption (Middle panel), the low doses specifically increase circulating levels of FGF21 which plays active roles in maintaining energy homeostasis, suppressing physical activity, and improving serum glucose levels in Pai/wt mice (Left panel). Conversely, the high doses specifically result in excesses of prostaglandin E2, corticosterone, glucagon, and CRP; subsequently, the combination of these factors causes metabolic syndrome, including hypothermia, fatty liver, and hypertriglyceridemia in Pai/Pai mice (Right panel). Words in black and red describe physiological features and endocrinal factors, respectively.

Our studies on male and female Pai mice suggest that the chronic effects of t10c12-CLA on lean animals are dose-dependent and differ between sexes. Furthermore, the metabolic impact of t10c12-CLA involves various hormones and has system-wide effects on multiple metabolic pathways. Thus, interpreting the data from Pai mice requires careful consideration, and more work is needed to understand the mechanism of action of t10c12-CLA and its metabolic impact.

Abbreviations

BAT, brown adipose tissue; CPT1, carnitine palmitoyltransferase 1; CRP, C-reactive protein; FA, fatty acids; FASN, fatty acid synthase; FGF21, fibroblast growth factor 21; IL-6, interleukin-6; LA, linoleic acid; pai, *Propionibacterium acnes* isomerase; (p)AMPK, phosphorylated AMP-activated protein kinase; PEG2, prostaglandin E2; (p)HSL, phosphorylated hormone-sensitive lipase; t10c12-CLA, *trans* 10, *cis* 12-conjugated linoleic acid; TC, total cholesterol; TGs, triglycerides; TNFα, tumour necrosis factor-alpha; UCP, uncoupling protein; WAT, white adipose tissue; wt, wild-type;

Ethics approval and consent to participate:

All animal experiments followed the Committee for Experimental Animals of Yangzhou University. All applicable institutional and/or national guidelines for the care and use of animals were followed.

Institutional Review Board Statement:

The animal study protocol was approved by the Ethics Committee of Yangzhou University (protocol code NSFC2020-SYXY-20 and dated 25 March 2020).

Consent for publication:

Not applicable

Availability of data and materials:

The datasets used and/or analysed during the current study are available from the corresponding author upon reasonable request.

Competing interests:

The authors declare that they have no competing interests.

Funding sources

This work was supported by the National Key Research and Development Program of China (2018YFC1003800), the Priority Academic Program Development of Jiangsu Higher Education Institutions (PAPD), and the Jiangsu Funding Program for Excellent Postdoctoral Talent.

Acknowledgement

We thank graduate students Qi Wang, Mei Liu, and Jiaqi Lu in our lab for their generous assistance in partial tests and Ms Yuyang Wang in our university for technique help in gas chromatography. We also thank Professor Hongjun Wang at the Medical University of South Carolina, USA, for the helpful discussion during the writing process and Ms Wenjing Gou's language assistance in preparing this manuscript.

Authors 'contributions:

Conceptualization, Y Rao and K Gou; Data curation, Y Rao, M Li, B Wang, Y Wang, and L Liang; Formal analysis, Y Rao and K Gou; Funding acquisition, Y Rao and K Gou; Investigation, Y Rao, M Li, B Wang, Y Wang and L Liang; Methodology, Y Rao, M Li, B Wang, Y Wang and L Liang; Project administration, K Gou; Software, Y Rao; Supervision, K Gou; Validation, K Gou; Visualization, Y Rao and L Liang; Writing – original draft, Y Rao; Writing – review & editing, K Gou. All authors proofread, made comments, and approved the report.

Supplementary data

This manuscript contains supplementary data.

References

[1] Shen W, Baldwin J, Collins B, Hixson L, Lee KT, Herberg T, et al. Low level of trans-10, cis-12 conjugated linoleic acid decreases adiposity and increases browning independent of inflammatory signaling in overweight Sv129 mice. Journal of Nutritional Biochemistry. 2015;26:616-25.

[2] den Hartigh LJ, Wang SR, Goodspeed L, Wietecha T, Houston B, Omer M, et al. Metabolically distinct weight loss by 10,12 CLA and caloric restriction highlight the importance of subcutaneous white adipose tissue for glucose homeostasis in mice. Plos One. 2017;12.

[3] Rao Y, Li SL, Li MJ, Wang BZ, Wang YY, Liang LW, et al. Transgenic mice producing the trans 10, cis 12-conjugated linoleic acid present reduced adiposity and increased thermogenesis and fibroblast growth factor 21 (FGF21). J Nutr Biochem. 2023:109419.

[4] Berkel C, Cacan E. Trans-10, cis-12 conjugated linoleic acid- and caloric restriction-mediated upregulation of CNDP2 expression in white adipose tissue in rodents, with implications in feeding and obesity. J Nutr Biochem. 2023;114:109269.

540 [5] Wang L, Zhang S, Huang Y, You W, Zhou Y, Chen W, et al. CLA improves the lipo-nutritional
541 quality of pork and regulates the gut microbiota in Heigai pigs. Food Funct. 2022;13:12093-104.

542 [6] Kanter JE, Goodspeed L, Wang S, Kramer F, Wietecha T, Gomes-Kjerulf D, et al. 10,12
543 Conjugated Linoleic Acid-Driven Weight Loss Is Protective against Atherosclerosis in Mice and Is
544 Associated with Alternative Macrophage Enrichment in Perivascular Adipose Tissue. Nutrients.
545 2018;10.

546 [7] Vaisar T, Wang S, Omer M, Irwin AD, Storey C, Tang C, et al. 10,12-Conjugated linoleic acid
547 supplementation improves HDL composition and function in mice. J Lipid Res. 2022;63:100241.

548 [8] Kim JH, Kim Y, Kim YJ, Park Y. Conjugated linoleic acid: Potential health benefits as a functional
549 food ingredient. Annu Rev Food Sci Technol. 2016;7:221-44.

550 [9] Marques TM, Wall R, O'Sullivan O, Fitzgerald GF, Shanahan F, Quigley EM, et al. Dietary trans-
551 10, cis-12-conjugated linoleic acid alters fatty acid metabolism and microbiota composition in mice.
552 Br J Nutr. 2015;113:728-38.

553 [10] Cuciniello R, Luongo D, Ferramosca A, Lunetti P, Rotondi-Aufiero V, Crispi S, et al. Conjugated
554 linoleic acid downregulates Alzheimer's hallmarks in aluminum mouse model through an Nrf2-
555 mediated adaptive response and increases brain glucose transporter levels. Free Radic Biol Med.
556 2022;191:48-58.

557 [11] Cordoba-Chacon J, Sugasini D, Yalagala PCR, Tummala A, White ZC, Nagao T, et al. Tissue-
558 dependent effects of cis-9,trans-11- and trans-10,cis-12-CLA isomers on glucose and lipid metabolism
559 in adult male mice. J Nutr Biochem. 2019;67:90-100.

560 [12] Clement L, Poirier H, Niot I, Bocher V, Guerre-Millo M, Krief S, et al. Dietary trans-10,cis-12
561 conjugated linoleic acid induces hyperinsulinemia and fatty liver in the mouse. J Lipid Res.
562 2002;43:1400-9.

563 [13] Kelley DS, Bartolini GL, Warren JM, Simon VA, Mackey BE, Erickson KL. Contrasting effects
564 of t10,c12- and c9,t11-conjugated linoleic acid isomers on the fatty acid profiles of mouse liver lipids.
565 Lipids. 2004;39:135-41.

566 [14] Jaudszus A, Moeckel P, Hamelmann E, Jahreis G. Trans-10,cis-12-CLA-caused lipodystrophy is
567 associated with profound changes of fatty acid profiles of liver, white adipose tissue and erythrocytes

568 in mice: possible link to tissue-specific alterations of fatty acid desaturation. Ann Nutr Metab.
569 2010;57:103-11.

570 [15] Letona AZ, Niot I, Laugerette F, Athias A, Monnot MC, Portillo MP, et al. CLA-enriched diet
571 containing t10,c12-CLA alters bile acid homeostasis and increases the risk of cholelithiasis in mice. J
572 Nutr. 2011;141:1437-44.

573 [16] Li SL, Ma SY, Xu BR, Fan ZY, Li MJ, Cao WG, et al. Effects of trans-10, cis-12-conjugated linoleic
574 acid on mice are influenced by the dietary fat content and the degree of murine obesity. Eur J Lipid
575 Sci Tech. 2015;117:1908-18.

576 [17] Flippo KH, Potthoff MJ. Metabolic Messengers: FGF21. Nat Metab. 2021;3:309-17.

577 [18] Subbaiah PV, Gould IG, Lal S, Aizezi B. Incorporation profiles of conjugated linoleic acid
578 isomers in cell membranes and their positional distribution in phospholipids. Biochim Biophys Acta.
579 2011;1811:17-24.

580 [19] Furuyashiki T, Narumiya S. Stress responses: the contribution of prostaglandin E(2) and its
581 receptors. Nat Rev Endocrinol. 2011;7:163-75.

582 [20] Zeigerer A, Sekar R, Kleinert M, Nason S, Habegger KM, Muller TD. Glucagon's metabolic
583 action in health and disease. Compr Physiol. 2021;11:1759-83.

584 [21] Saper CB, Lowell BB. The hypothalamus. Curr Biol. 2014;24:R1111-6.

585 [22] Cypess AM, Weiner LS, Roberts-Toler C, Franquet Elia E, Kessler SH, Kahn PA, et al. Activation
586 of human brown adipose tissue by a beta3-adrenergic receptor agonist. Cell Metab. 2015;21:33-8.

587 [23] Contreras C, Gonzalez-Garcia I, Seoane-Collazo P, Martinez-Sanchez N, Linares-Pose L, Rial-
588 Pensado E, et al. Reduction of hypothalamic endoplasmic reticulum stress activates browning of
589 white fat and ameliorates obesity. Diabetes. 2017;66:87-99.

590 [24] Contreras C, Fondevila MF, Lopez M. Hypothalamic GRP78, a new target against obesity?
591 Adipocyte. 2018;7:63-6.

592 [25] Martins L, Seoane-Collazo P, Contreras C, Gonzalez-Garcia I, Martinez-Sanchez N, Gonzalez
593 F, et al. A functional link between ampk and orexin mediates the effect of bmp8b on energy balance.
594 Cell Rep. 2016;16:2231-42.

595 [26] Chemelli RM, Willie JT, Sinton CM, Elmquist JK, Scammell T, Lee C, et al. Narcolepsy in orexin
596 knockout mice: Molecular genetics of sleep regulation. Cell. 1999;98:437-51.

597 [27] Ashwell MS, Ceddia RP, House RL, Cassady JP, Eisen EJ, Eling TE, et al. Trans-10, cis-12-
598 conjugated linoleic acid alters hepatic gene expression in a polygenic obese line of mice displaying
599 hepatic lipidosis. J Nutr Biochem. 2010;21:848-55.

600 [28] Vyas D, Kadegowda AK, Erdman RA. Dietary conjugated linoleic acid and hepatic steatosis:
601 species-specific effects on liver and adipose lipid metabolism and gene expression. J Nutr Metab.
602 2012;2012:932928.

603 [29] Laryea G, Schutz G, Muglia LJ. Disrupting hypothalamic glucocorticoid receptors causes HPA
604 axis hyperactivity and excess adiposity. Mol Endocrinol. 2013;27:1655-65.

605 [30] Nicolaides NC, Charmandari E, Kino T, Chrousos GP. Stress-related and circadian secretion
606 and target tissue actions of glucocorticoids: Impact on health. Front Endocrinol (Lausanne).
607 2017;8:70.

608 [31] Krilov L, Nguyen A, Miyazaki T, Unson CG, Bouscarel B. Glucagon receptor recycling: role of
609 carboxyl terminus, beta-arrestins, and cytoskeleton. Am J Physiol-Cell Ph. 2008;295:C1230-C7.

610 [32] Charbonneau A, Unson CG, Lavoie JM. High-fat diet-induced hepatic steatosis reduces glucagon
611 receptor content in rat hepatocytes: potential interaction with acute exercise. J Physiol-London.
612 2007;579:255-67.

613 [33] Sammons MF, Lee ECY. Recent progress in the development of small-molecule glucagon receptor
614 antagonists. Bioorg Med Chem Lett. 2015;25:4057-64.

615 [34] Perry RJ, Zhang D, Guerra MT, Brill AL, Goedeke L, Nasiri AR, et al. Glucagon stimulates
616 gluconeogenesis by INSP3R1-mediated hepatic lipolysis. Nature. 2020;579:279-83.

617 [35] Hayashi Y. Glucagon regulates lipolysis and fatty acid oxidation through inositol triphosphate
618 receptor 1 in the liver. J Diabetes Investig. 2021;12:32-4.

619 [36] Kleinert M, Sachs S, Habegger KM, Hofmann SM, Muller TD. Glucagon regulation of energy
620 expenditure. Int J Mol Sci. 2019;20.

621 [37] Schlein C, Talukdar S, Heine M, Fischer AW, Krott LM, Nilsson SK, et al. Fgf21 lowers plasma
622 triglycerides by accelerating lipoprotein catabolism in white and brown adipose tissues. Cell Metab.
623 2016;23:441-53.

624 [38] Bookout AL, de Groot MH, Owen BM, Lee S, Gautron L, Lawrence HL, et al. FGF21 regulates
625 metabolism and circadian behavior by acting on the nervous system. Nat Med. 2013;19:1147-52.

626 [39] Holland WL, Adams AC, Brozinick JT, Bui HH, Miyauchi Y, Kusminski CM, et al. An FGF21-
627 adiponectin-ceramide axis controls energy expenditure and insulin action in mice. Cell Metab.
628 2013;17:790-7.

629 [40] Henriksen EJ, Teachey MK, Taylor ZC, Jacob S, Ptock A, Kramer K, et al. Isomer-specific actions
630 of conjugated linoleic acid on muscle glucose transport in the obese Zucker rat. Am J Physiol
631 Endocrinol Metab. 2003;285:E98-E105.

632 [41] Tsuboyama-Kasaoka N, Takahashi M, Tanemura K, Kim HJ, Tange T, Okuyama H, et al.
633 Conjugated linoleic acid supplementation reduces adipose tissue by apoptosis and develops
634 lipodystrophy in mice. Diabetes. 2000;49:1534-42.

635